Experimental Neurology 340 (2021) 113656

Contents lists available at ScienceDirect

Experimental Neurology

journal homepage: www.elsevier.com/locate/yexnr

Research paper

Dexamethasone-induced activation of heat shock response ameliorates seizure susceptibility and neuroinflammation in mouse models of Lafora disease

Priyanka Sinha, Bhupender Verma, Subramaniam Ganesh *

Department of Biological Sciences and Bioengineering, Indian Institute of Technology, Kanpur, India

ARTICLE INFO

Keywords:
Epilepsy
Stress response
Inflammation
Neurodegeneration
Mouse models

ABSTRACT

Heat shock response (HSR) is a conserved cytoprotective pathway controlled by the master transcriptional regulator, the heat shock factor 1 (HSF1), that activates the expression of heat shock proteins (HSPs). HSPs, as chaperones, play essential roles in minimizing stress-induced damages and restoring proteostasis. Therefore, compromised HSR is thought to contribute to neurodegenerative disorders. Lafora disease (LD) is a fatal form of neurodegenerative disorder characterized by the accumulation of abnormal glycogen as Lafora bodies in neurons and other tissues. The symptoms of LD include progressive myoclonus epilepsy, dementia, and cognitive deficits. LD is caused by the defects in the gene coding laforin phosphatase or the malin ubiquitin ligase. Laforin and malin are known to work upstream of HSF1 and are essential for the activation of HSR. Herein, we show that mice deficient for laforin or malin show reduced levels of HSF1 and their targets in their brain tissues, suggesting compromised HSR; this could contribute to the neuropathology in LD. Intriguingly, treatment of LD animals with dexamethasone, a synthetic glucocorticoid analogue, partially restored the levels of HSF1 and its targets. Dexamethasone treatment was also able to ameliorate the neuroinflammation and susceptibility to induced seizures in the LD animals. However, dexamethasone treatment did not show a significant effect on Lafora bodies or autophagy defects. Taken together, the present study establishes a role for HSR in seizure susceptibility and neuroinflammation and dexamethasone as a potential antiepileptic agent, suitable for further studies in LD.

1. Introduction

Heat shock response (HSR) is a conserved cellular stress response pathway that protects cells from a variety of stressors, including heat shock (Goenka et al., 2018). HSR is controlled by a master regulator, the heat shock factor 1 (HSF1), a highly conserved transcription factor. On exposure to heat stress, HSF1 activates the overexpression of a set of genes involved in cytoprotective stress response mechanisms (Verghese et al., 2012; Le Breton and Mayer, 2016; Dai, 2018). One of the major functions of these proteins, collectively known as the heat shock proteins (HSPs), is to prevent the aggregation of stress-induced unfolded proteins and help in their refolding (Tonkiss and Calderwood, 2005; Vabulas et al., 2010; Saibil, 2013). Defects in this process or chronic stress may lead to the activation of cell death pathways (Creagh et al., 2000; Beere, 2004; Kennedy et al., 2014). Besides its cytoprotective role against transient stress, HSR is also known to play a role in systemic conditions such as aging, cardiovascular disease, autoimmune disorders, and neurodegenerative disorders (Pockley, 2002; Calderwood et al., 2009; Kakkar et al., 2014; Tukaj and Kaminski, 2019). Amongst these, the neurodegenerative disorders represent a prominent group of ailments that often associate with abnormal protein folding and aggregation (Leak, 2014; Sweeney et al., 2017). Therefore, compromised proteostasis is thought to underlie neurodegeneration in such conditions. Indeed, components of proteostasis systems were found to be associated with the neurotoxic protein aggregates (Cummings et al., 1998; Jana et al., 2000), and in some cases, to be deficient in neurons (Kato et al.,

Abbreviations: HSR, heat shock response; HSF1, heat shock factor 1; LD, Lafora disease; LBs, Lafora bodies; LKO, laforin knockout; MKO, malin knockout; HSPs, heat shock proteins; GFAP, glial fibrillary acidic protein; Iba1, ionized calcium-binding adaptor molecule 1; SOD1, superoxide dismutase 1; PTZ, pentylenetetrazol; UPR, unfolded protein response; PAS staining, periodic acid-Schiff staining; RT-PCR, real time polymerase chain reaction; ANOVA, analysis of variance; SEM, standard error of the mean.

* Corresponding author at: Department of Biological Sciences and Bioengineering, Indian Institute of Technology, Kanpur 208016, India.
E-mail address: sganesh@iitk.ac.in (S. Ganesh).

https://doi.org/10.1016/j.expneurol.2021.113656
Received 6 September 2020; Received in revised form 26 January 2021; Accepted 21 February 2021
Available online 24 February 2021

1999; Warrick et al., 1999; Wyttenbach et al., 2002; Howarth et al., 2007). Thus, the deficiency in proteostasis, either directly or indirectly, appears to contribute to the pathology in neurodegenerative disorders (Mittal and Ganesh, 2010). Indeed, experimental overexpression of heat shock proteins was shown to delay or rescue neurodegeneration in the animal models (Hansson et al., 2003). Similar observations were made when pharmacological activation of HSF1 was attempted (Maheshwari et al., 2014), suggesting that HSR plays an important role in neuroprotection.

The progressive myoclonus epilepsy of Lafora or the Lafora disease (LD), as it is popularly called, is an inherited neurodegenerative disorder (Singh and Ganesh, 2009; Parihar et al., 2018). The symptoms of LD include myoclonic seizures, ataxia, psychosis, and dysarthria (Striano et al., 2008; Singh and Ganesh, 2009). A major pathological hallmark of LD is the accumulation of carbohydrate-rich inclusions known as Lafora bodies in multiple tissues including the neurons, muscle, and liver (Tagliabracci et al., 2007; Turnbull et al., 2016). LD manifests as epilepsy in early adolescence, and the patients quickly develop the other symptoms with death ensuing in about 10 years after the onset (Turnbull et al., 2012). LD is caused by defects in the *EPM2A* gene coding for a dual-specificity protein phosphatase named laforin or the *NHLRC1* gene coding for an E3 ubiquitin ligase named malin (Minassian et al., 1998; Ganesh et al., 2000; Chan et al., 2003; Gentry et al., 2005;). Laforin and malin are shown to work in multiple cellular pathways, including the proteostasis (Mittal et al., 2007; Garyali et al., 2009; Aguado et al., 2010; Garyali et al., 2014). Specifically, the laforin-malin complex promotes degradation of misfolded proteins (Mittal et al., 2007; Garyali et al., 2009), induces autophagy (Aguado et al., 2010; Puri et al., 2012; Singh et al., 2013) and unfolded protein response (Garyali et al., 2009; Aguado et al., 2010; Garyali et al., 2014). We have shown earlier that laforin and malin are essential for the cell to mount an effective response against heat stress (Sengupta et al., 2011) and activate HSF1 during heat stress (Jain et al., 2017). Thus, compromised HSF1-mediated HSR might contribute to neuropathology and associated symptoms in LD. To test this possibility, we have used mouse models of LD – animals that are deficient for either laforin or malin. We demonstrate here that dexamethasone induced HSR increases HSP levels and ameliorates seizure susceptibility and neuroinflammation in LD mouse models.

2. Materials and methods

2.1. Chemicals and antibodies

The following chemicals and reagents were used for this study: Dexamethasone (Cat. No. D2915), pentylenetetrazol (Cat. No. P6500), 1× protease inhibitor cocktail (Cat. No. P2714), Triton X-100 (Cat. No. T8787) (all from Sigma-Aldrich Chemicals Pvt. Ltd., India), trizol reagent (Cat. No. 15596026), periodic acid (Cat. No. 19184), RiboLock RNase inhibitor (Cat. No. EO0381), Reverse Transcriptase (Cat. No. EP0352) (all from Thermo Fisher Scientific India Pvt. Ltd.), Schiff's reagent (Cat. No. 141407; Thomas Baker Chemicals Pvt. Ltd. India), α-amylase (Cat. No. 28588), hematoxylin (Cat. No. 48441) (all from Sisco Research Laboratories Pvt. Ltd., India), donkey serum (Cat. No. S30), DPX (Cat. No. 61803502501730) (all from Merck, India), DAB chromogen kit (Cat. No. 1610500011730; Bangalore Genei Pvt. Ltd., India), 1× phosphatase inhibitor cocktail (Cat. No. 4906845001; Roche Products India Pvt. Ltd.), and nitrocellulose membrane (Cat. No. 1620112; Bio-Rad laboratories India Pvt. Ltd.). Following antibodies were used for the experiments: anti-GFAP (Cat. No. ab7260; Abcam U.S.A) (dilution: IB – 1:1000; IHC – 1:500), anti-Iba1 (Cat. No. ab5076; Abcam, U.S.A) (dilution: IB – 1:1000; IHC – 1:500 dilution), anti-γ-tubulin (Cat. No. T5326; Sigma-Aldrich Chemicals Pvt. Ltd., India) (dilution: IB – 1:10,000), anti-LC3 (Cat. No. L7543; Sigma-Aldrich Chemicals Pvt. Ltd., India) (dilution: IB - 1:1000), anti-SOD1 (Cat. No. 4266S; Cell Signaling Technology Inc., U.S.A) (dilution: IB – 1:1000), anti-p62 (Cat. No. 5114S; Cell Signaling Technology Inc., U.S.A) (dilution: IB – 1:1000), anti-HSF1 (Cat. No. 4356S; Cell Signaling Technology Inc., U.S.A) (dilution: IB – 1:1000), anti-HSP70 (Cat. No. 4872S; Cell Signaling Technology Inc., U.S.A) (dilution: IB – 1:1000), and anti-HSP90 (Cat. No. 4874S; Cell Signaling Technology Inc., U.S.A) (dilution: IB – 1:1000).

2.2. Mice and drug administration

Two different lines of Lafora disease mouse models were used in the present study. They were laforin-knockout mouse (LKO) (Ganesh et al., 2002) and malin-knockout mouse (MKO) (Pederson et al., 2013), and both lines were obtained from Dr. Berge Minassian (Hospital for Sick Children, Ontario, Canada). The animal experiments were approved by the Institutional Animal Ethics Committee of IIT Kanpur and experiments were conducted in accordance with guidelines proposed by the Committee for the Purpose of Control and Supervision of Experiments on Animals, Govt. of India. Animals were maintained in the in-house institute facility on a 12/12 light/dark cycle in regulated temperature (25 °C) with *ad libitum* access to food and water. For the study, homozygous null mutants and their wild-type littermates derived from the cross set between heterozygous mice were used. For the treatment, six-month-old mice were subcutaneously injected with dexamethasone at the dosage of 4 mg/kg/alternate day for a duration of two months. Littermates injected with an equal volume of sterile saline (vehicle) served as control.

2.3. Pentylenetetrazol (PTZ)-induced seizures scoring

Eight-month-old animals, treated with dexamethasone or vehicle, were intraperitoneally injected with PTZ (45 mg/kg body weight) to induce seizures. Injected animals were videotaped for 30 min. Seizures were scored by a user blinded to the genotype and treatment of animals by reviewing video files. The time spent by each mouse in all stages of seizure was recorded, and the latency, severity, and duration of seizures for control and treated mice were calculated. We used a modified Racine scale to calculate the severity of seizures. Each stage of seizure was given weightage while calculating latency and duration of seizures, as explained in detail in the supporting information.

2.4. Periodic Acid-Schiff (PAS) staining

Periodic Acid-Schiff (PAS) staining was performed on tissue sections, as described earlier (Mitsuno et al., 1999; Ganesh et al., 2002). Paraformaldehyde-fixed brain tissues were embedded in paraffin. For PAS staining, 5 μm sections were cut, deparaffinized using xylene and hydrated using a graded series of ethanol (100%, 95%, 75%, 50%, and 25%). These sections were then treated with 1 mg/mL amylase at 37 °C for 5 min and washed with autoclaved water. The sections were then oxidized using periodic acid solution (1% *w/v*) for 20 min at room temperature and rinsed thrice with autoclaved water. The sections were then incubated with Schiff's reagent for 10 min at room temperature and then washed with water. They were then counterstained with hematoxylin and dehydrated. Dehydrated slides were then mounted in DPX and visualized under a brightfield microscope at 400× magnification.

2.5. Immunohistochemistry

Immunohistochemistry for paraffin-embedded brain sections was carried out essentially as described before (Rai et al., 2017). For this, 5 μm brain sections were cut and hydrated using graded series of alcohol. For antigen retrieval, sections were boiled in Tris-EDTA buffer (Tris 10 mM, EDTA 0.5 mM, pH 9.0) for 30 min. The sections were kept in the same buffer and were allowed to cool down to room temperature and then they were washed with 1× TBST (Tris 20 mM, NaCl 150 mM, 0.025% Triton X-100). The sections were then permeabilized using 0.2% Triton X-100 (*v*/v in 1× TBST) for 20 min and incubated sequentially

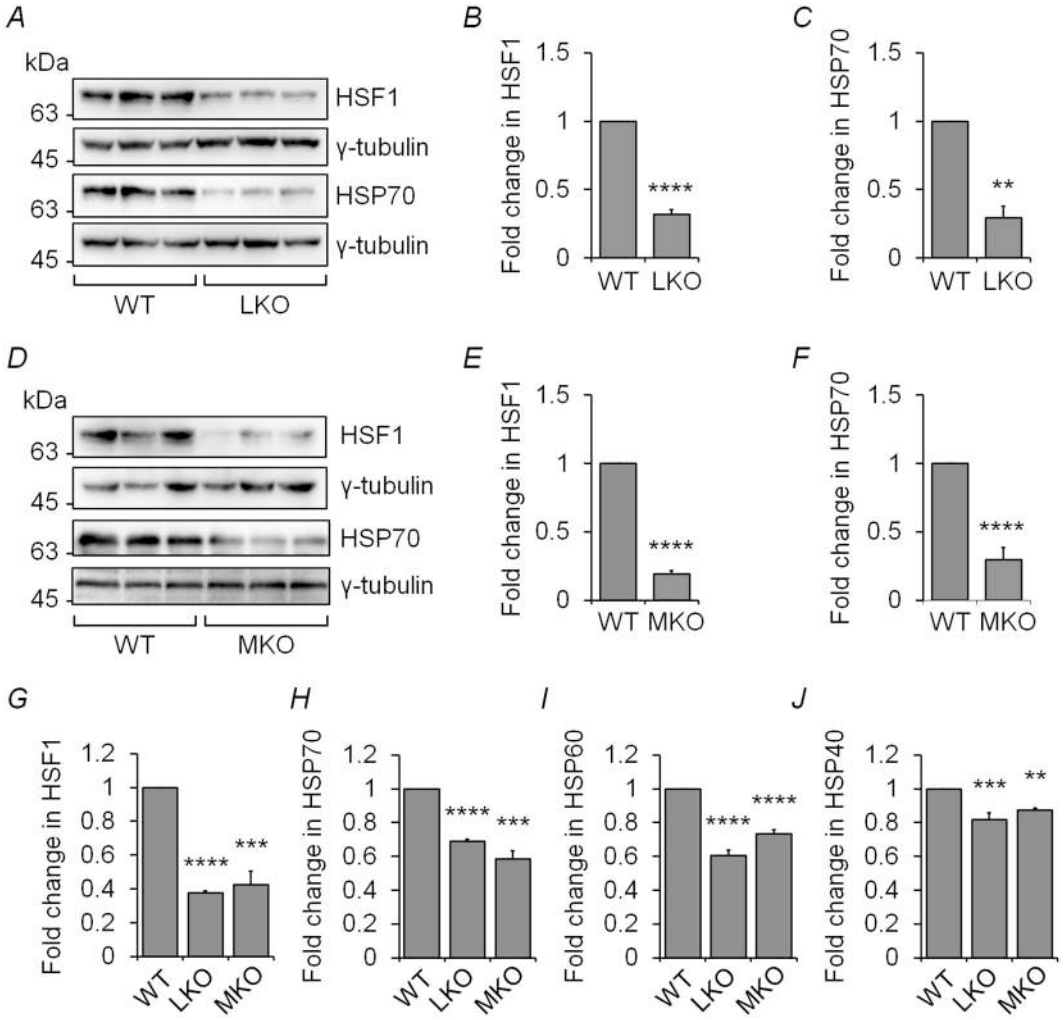

Fig. 1. HSF1 is downregulated in the LD mice brains.

Representative images of immunoblots showing the reduced levels of HSF1 and one of its target gene protein (HSP70) in the whole brain tissue lysates from laforin- (LKO) (***A***) or malin-deficient mice (MKO) (***D***) as compared to wild-type (WT) littermates, as indicated. Bar diagrams show the relative signal intensities of the HSF1 and HSP70 immunoreactive bands, normalized to γ -tubulin bands, and plotted for laforin-deficient mice (***B*** and ***C***) or malin-deficient (***E*** and ***F***) mice as compared to their wild-type littermates. Each bar represents the mean average (+ SEM); Student's unpaired *t*-test was used to calculate the significance; asterisks denote statistically significant changes where ** $p < 0.01$, **** $p < 0.0001$, $n = 3$. (***G–J***) Bar diagrams showing the fold change in the level of transcripts for HSF1, HSP70, HSP60, and HSP40 in the whole brain lysates of laforin- (LKO) or malin-deficient mice (MKO) as compared to their wild-type littermates (WT), as indicated. Each bar represents the mean average (+ SEM); the statistical significance was calculated using an ordinary one-way ANOVA test ($n = 6$; asterisks denote statistically significant changes where ** $p < 0.01$, *** $p < 0.001$, and **** $p < 0.0001$).

with first blocking buffer (50% donkey serum; v/v in 1× TBST) for 30 min and second blocking buffer (10% donkey serum; v/v in 1× TBST) for 90 min. Sections were then incubated with primary antibody diluted (as per manufacturer's recommendation) in 10% donkey serum overnight at 4 °C in a moist chamber. They were then washed with 1× TBST twice followed by incubation with 0.3% H_2O_2 (v/v in 1× TBST) for 15 min and incubated with HRP-tagged secondary antibody (diluted in 1× TBST) for an hour at room temperature. The immuno-positive signals were developed using DAB conjugated avidin-biotin complex kit (Vectastain ABC Elite, Vector Laboratories, USA) and visualized using a brightfield microscope at 400× magnification.

2.6. Image acquisition and analysis

Images of the sections were acquired using the Nikon ECLIPSE 80i microscope mounted with the Nikon DS-Fi3 camera. For the quantification of PAS-positive inclusions, stained sections were imaged with a 40× oil objective lens. The total number of Lafora bodies were quantified, and the number was divided by the total area and expressed as number/mm^2. All images were analyzed using ImagePro (Version 6.3) of Media Cybernetics.

For immunohistological studies, microscopic images were acquired using Nikon ECLIPSE 80i microscope using a 40× oil objective by a user blinded to the genotype and treatment groups. For quantification, we have used five images for a given region from a brain section, three sections were used for each brain, and four brains for each study group were included for the study. ImageJ software was used to quantify the pixel intensity of immunostained area. Briefly, the acquired images were converted to an 8-bit greyscale, a fixed threshold for intensity was set, and the number of pixels from each section was quantified. The number of pixels obtained from each section were normalized to the total area of each image to get final values in pixels/μm^2. The mean of the values thus obtained (in pixels/μm^2) from each microscopic field from each group were used for statistical analyses.

2.7. RNA extraction and Real-Time PCR

Whole brains were homogenized in Trizol reagent and precipitated

using isopropanol. The precipitated RNA was then dissolved in RNase free autoclaved water and processed for cDNA synthesis. Reverse transcription reactions were set up by initially mixing RNA (2 μg) and random primers (0.2 μg) in RNase free autoclaved water and incubating this mix at 70 °C for 5 min followed by snap-freezing for 5 min. The following were then added: RiboLock RNase inhibitor, 5× reverse transcriptase reaction buffer, dNTP mix (10 mM) and reverse transcriptase. The reaction was incubated at 25 °C for 5 min, 42 °C for 90 min, and 70 °C for 10 min. The resulting cDNA was used to quantitate the relative expression of all targets using Luna Universal qPCR Master Mix as per the manufacturer's recommendation (New England Biolabs Pvt. Ltd., India). Primer sequences used for amplification are listed in Supplementary Material Table S1.

2.8. Immunoblotting

Whole brain lysates were prepared by homogenizing the brain tissue in a 1× RIPA buffer supplemented with a 1× protease inhibitor cocktail and a 1× phosphatase inhibitor cocktail. An equal amount of protein was loaded and size separated through sodium dodecyl sulfate-polyacrylamide gel electrophoresis. Protein samples were then transferred onto a nitrocellulose membrane, and the membrane was incubated with primary and secondary antibodies as recommended by the manufacturer. Immunoreactive bands were visualized using a chemiluminescence kit (Thermo Fisher Scientific India Pvt. Ltd.), and images were captured using ChemiDoc XRS+ (Bio-Rad Laboratories India Pvt. Ltd). Signal intensities were quantified using ImageJ software (NIH, USA).

2.9. Statistical analysis

All values are mentioned as mean + SEM as derived from at least three independent experiments. Student's unpaired *t*-test or ordinary one-way ANOVA was performed to calculate the significance of normally distributed data. For ordinal data, Kruskal-Wallis ANOVA on the RANKS test was used to assess the statistical significance. Statistical significance was considered at ****, $p < 0.0001$; ***, $p < 0.001$; **, $p < 0.01$; *, $p < 0.05$ or ####, p < 0.0001; ###, p < 0.001; ##, p < 0.01; #, $p < 0.05$. GraphPad Prism software was used for statistical analyses.

3. Results

3.1. HSF1 is reduced in Lafora disease mice brains

Since laforin and malin are known to regulate the activity of HSF1 (Sengupta et al., 2011), and since HSR is known to be compromised in the degenerating brain (Hay et al., 2004; Yamanaka et al., 2008; Maheshwari et al., 2014), we wanted to check the level of HSF1 and its targets in the brain tissue of LD mouse models. We, therefore, measured the level of HSF1 and one of its targets, HSP70, by immunoblotting in the whole brain lysates of laforin- and malin-deficient mice. As shown in Fig. 1A–F, there was a significant reduction in the levels of HSF1 as well as HSP70 in the knockout mice. Next, we wanted to check if the level difference can also be seen in the transcripts. For this, we used the real-time polymerase chain reaction (RT-PCR) method to measure the transcript levels. As shown in Fig. 1G–J, the levels of HSF1 and three of its targets HSP70, HSP60, and HSP40 were significantly lower in the brain tissues of the laforin- and malin-deficient mice. Taken together, these observations suggest that the HSR pathway is compromised in mouse models of LD.

3.2. Dexamethasone treatment increases the levels of HSF1 and its targets in LD mice

Dexamethasone, a steroid, is known to activate HSF1 and HSF1-mediated HSR in cell lines and animals (Sun et al., 2000; Knowlton and Sun, 2001; Maheshwari et al., 2014). Therefore, we wanted to check if dexamethasone treatment can restore HSF1 level or functions in the LD mouse models. For this, six-month-old animals were treated with dexamethasone (4 mg/kg/alternate day) for two months, and then the transcript levels of HSF1 and its targets were measured. As shown in Fig. 2A, dexamethasone treatment resulted in a significant increase in the HSF1 transcript level in LD mice brains as compared to untreated controls. A similar effect was seen for three HSF1 targets tested except for HSP40 in malin-deficient mice (Fig. 2B–D). Since dexamethasone is an HSP90 inhibitor, it could reduce the protein levels of HSP90 in dexamethasone-treated mice brain. Therefore, we also investigated the protein levels of HSP90, HSF1, and HSP70 by immunoblotting and found a significant increase in their levels after dexamethasone treatment (Fig. 3 and Supplementary Fig. S1). Hence, we conclude that dexamethasone could partially restore the HSR pathway in LD mouse models.

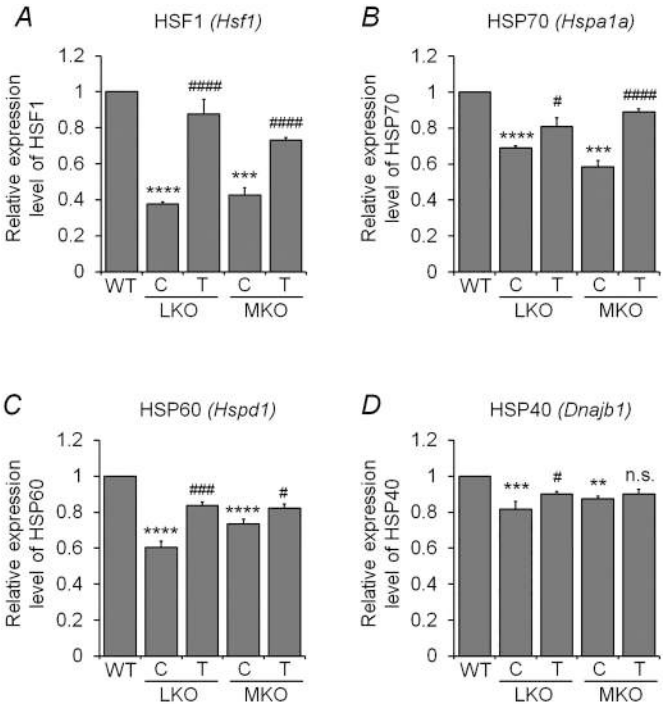

Fig. 2. Dexamethasone treatment increases the expression levels of HSF1 and its targets in LD mice.
Bar diagram showing the fold change in the expression levels of genes coding for HSF1 (***A***), HSP70 (***B***), HSP60 (***C***), and HSP40 (***D***) in the whole brain tissues of laforin- (LKO) or malin-deficient mice (MKO) that were treated (identified as "[T]") with dexamethasone, as compared to the wild-type (WT) animals or the vehicle treated controls (identified as "[C]"). Each bar represents the mean average (+ SEM); the statistical significance was calculated using an ordinary one-way ANOVA test (n = 6). Herein, asterisk refers to comparison with the wild-type untreated samples (** p < 0.01; *** p < 0.001; **** p < 0.0001), and the hashtag refers to the comparison with the control sets (vehicle-treated; [C]) of the respective genotypes (# $p < 0.05$; ### p < 0.001; ####p < 0.0001).

3.3. Dexamethasone ameliorates neuroinflammation in LD mice

Neuroinflammation is one of the hallmarks of Lafora disease pathology (Turnbull et al., 2011; Puri et al., 2012; Turnbull et al., 2014; López-González et al., 2017) as shown in Supplementary Figs. S2–S3. Since the HSR pathway is known to modulate neuroinflammation (Dukay et al., 2019), and dexamethasone is an established steroidal anti-inflammatory drug (Knop et al., 2012), we next explored if dexamethasone treatment would ameliorate neuroinflammation in LD mice. To test this, we looked at the distribution of two major markers of glial

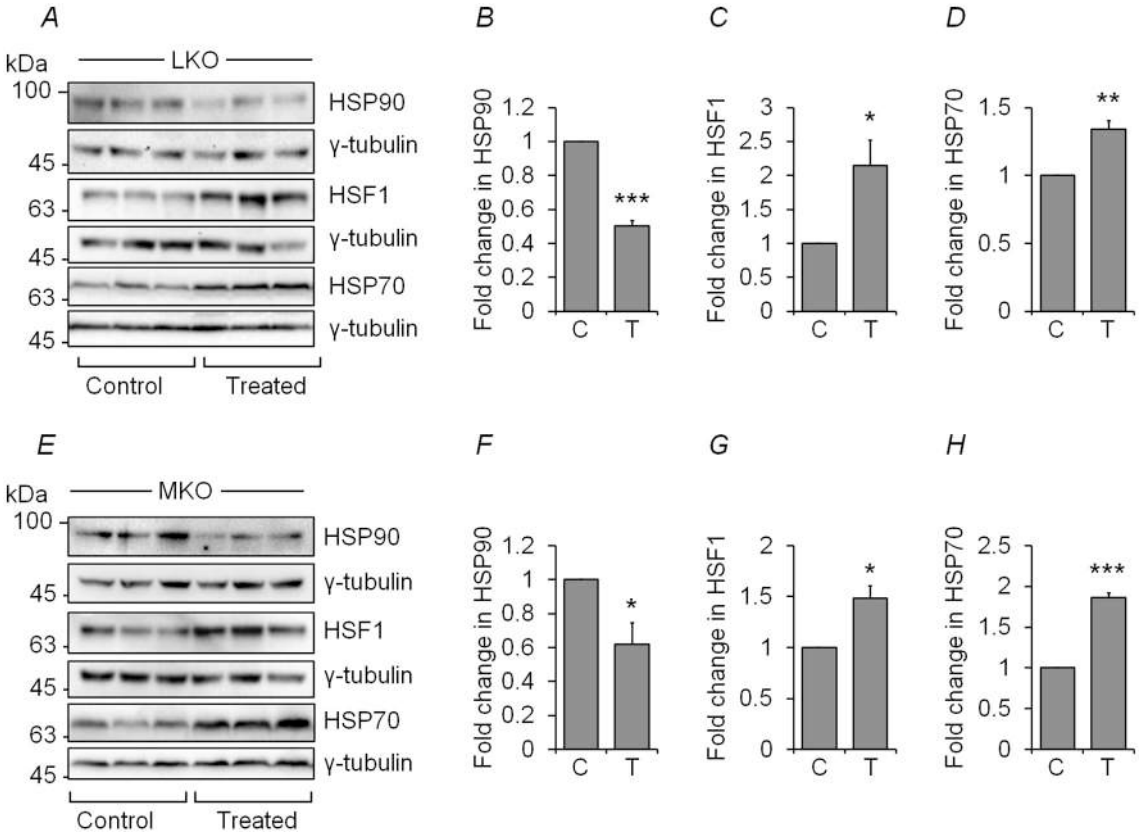

Fig. 3. Dexamethasone induces HSF1 by inhibiting HSP90 in LD mice brains Representative images of the immunoblots showing relative levels of HSP90, HSF1, HSP70, and the loading control (γ -tubulin) in the whole brain lysate of the laforin-deficient animals (LKO) (*A*) or the malin-deficient animals (MKO) (*E*) either as vehicle treated controls (identified as "[C]") or upon dexamethasone-treated (identified as "[T]") as identified. The bar diagrams (*B*, *C*, *D*, *F*, *G*, and *H*) show the fold change in signal intensity for the immunoreactive bands for HSP90, HSF1 and HSP70 (measured by densitometric analysis) in the dexamethasone-treated samples (identified as "[T]") as compared to the vehicle treated controls (identified as "[C]") of respective genotypes. The signals were normalized to the γ-tubulin level. Each bar represent the mean average (+ SEM), and the statistical significance was calculated using Student's unpaired t-test (n = 3); asterisks denote statistically significant changes where * $p < 0.05$, ** $p < 0.01$, and *** $p < 0.001$.

activation, the glial fibrillary acidic protein (GFAP) and ionized calcium-binding adaptor molecule 1 (Iba1), by immunohistochemical approach. Since GFAP shows high expression in the CA1 region, the CA1 region was used for the image analysis. Conversely, Iba1 shows expression throughout the brain, hence cortices were also included for the analyses. As shown in Fig. 4 and Supplementary Figs. S4–S7, dexamethasone treatment resulted in a significant reduction in the glial activation in both laforin- and malin-deficient mice. We also checked the transcript levels of four neuroinflammation markers (*Gfap, Iba1, Tnfa,* and *Ptgs2*). As shown in Fig. 5A–D dexamethasone treatment partially restored the expression levels of all four genes tested. The protein levels of two of the markers (GFAP and Iba1) were also checked, by immunoblotting, in the whole brain lysates of dexamethasone-treated knockout and control mice. As shown in Fig. 5E–J, dexamethasone treatment led to significant reduction in the levels of GFAP and Iba1 in the whole brain lysates of the LD mice. Taken together, our data suggest that dexamethasone treatment was able to suppress inflammation in LD mice brain.

3.4. Dexamethasone reduces oxidative stress in LD mice brain

Since the LD brain is known to show increased oxidative stress (Romá-Mateo et al., 2015a; Romá-Mateo et al., 2015b), and HSF1 is known to play a causal role in the oxidative stress response (Barna et al., 2018), we were also interested in checking if dexamethasone treatment would suppress the oxidative stress in LD brains. For this, we looked at the level of superoxide dismutase 1 (SOD1) in the brain tissues by immunoblotting. As shown in Fig. 6A–D, the level of SOD1 in the whole brain lysates of LD mice was significantly higher. Moreover, treatment with dexamethasone resulted in a significant reduction in the SOD1 level in LD brains (Fig. 6E–H).

3.5. Dexamethasone ameliorates susceptibility to induced seizures in LD mice

One of the major hallmarks of LD is the onset of epileptic seizures. While animal models of LD did develop spontaneous seizures (Ganesh et al., 2002; Turnbull et al., 2010; García-Cabrero et al., 2012), their penetrance and duration were much milder as compared to what is seen in humans (Ganesh et al., 2002). However, the LD animals were shown to have a lower threshold for chemically induced epilepsy (García-Cabrero et al., 2014; Rai et al., 2017; Sinha et al., 2020). Pentylenetetrazol-induced seizures (PTZ) is one of the commonly used assays to test seizure susceptibility in LD; therefore, we checked if dexamethasone treatment alters the duration, latency, and/or severity for the PTZ-induced seizures. As shown in Fig. 7A–B, the dexamethasone-treated animals showed a significant reduction in the duration as well as severity for the PTZ-induced seizures. However, there was no change observed in the latency (the time taken to reach

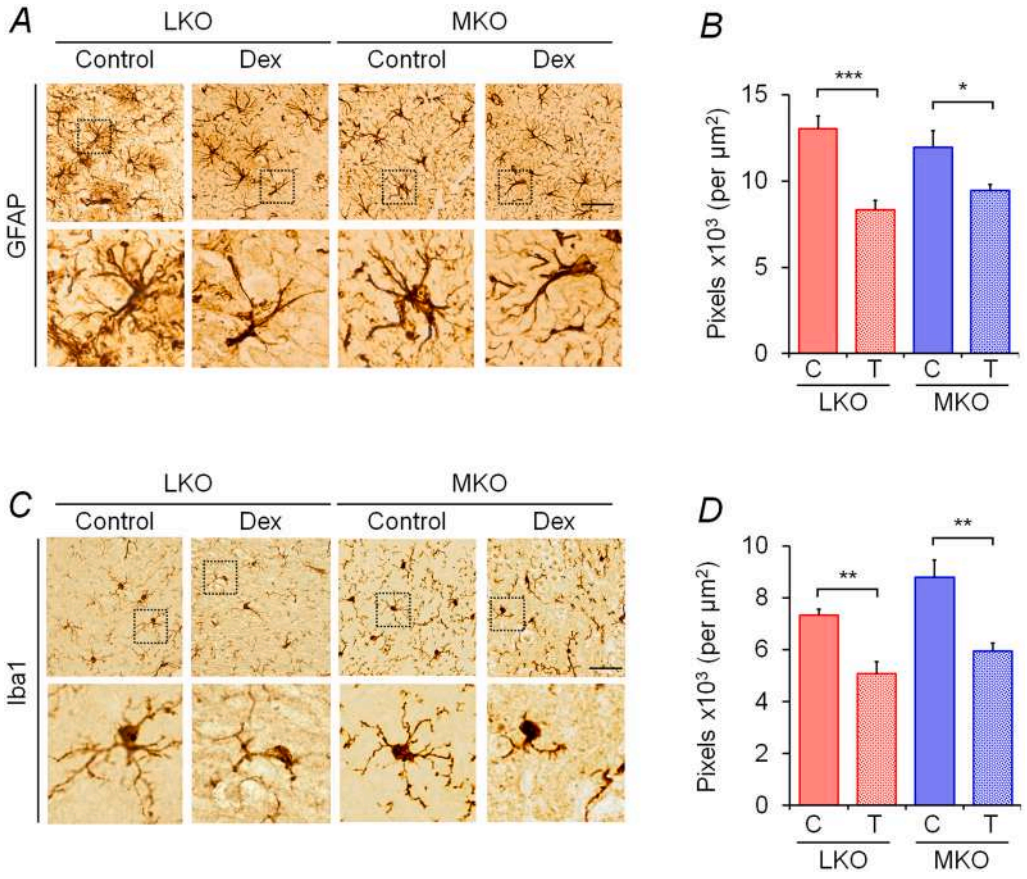

Fig. 4. Dexamethasone treatment reduces gliosis in LD mice brains. Representative brightfield microscopic images from the brain sections showing the distribution of the GFAP (***A***) or Iba1 (***C***) positive cells in the CA1 region of hippocampus of laforin- (LKO) or malin-deficient (MKO) mice that were vehicle treated (control) or treated with dexamethasone (Dex), as indicated (scale bar = 50 µm). The inset represents the area that is magnified in the lower panel. The bar diagrams (***B*** and ***D***) represent the number of pixels of GFAP or Iba1 staining per unit area ($n = 4$; Ordinary one-way ANOVA; * $p < 0.05$, ** $p < 0.01$, and *** $p < 0.001$).

each seizure stage) observed (Fig. 7C). These observations perhaps imply that while dexamethasone did not influence the threshold time for induction of each seizure stage; however, it could reduce the severity and duration of seizures.

3.6. *Dexamethasone treatment has no effect on Lafora bodies*

Lafora bodies are the disease defining neuropathological hallmarks of LD. Studies have shown that suppression of Lafora bodies ameliorates neuropathology and suppresses seizure susceptibility (Turnbull et al., 2011; Turnbull et al., 2014). Therefore, we looked at the distribution of Lafora bodies in the dexamethasone-treated LD animals. As shown in Fig. 8, dexamethasone treatment did not have a significant effect on the size and distribution of Lafora bodies in the brain tissues as compared to controls.

3.7. *Dexamethasone treatment has no effect on autophagy*

Since autophagy defects are well documented in LD (Aguado et al., 2010; Criado et al., 2012; Puri et al., 2012) and since dexamethasone is known to induce autophagy in a dosage-dependent manner (Laane et al., 2009; Molitoris et al., 2011; Zhou et al., 2019), we next tested if dexamethasone restores autophagy in LD animals. For this, we looked at the levels of two established autophagy markers - p62 and LC3II - in whole brain lysates using immunoblotting. As shown in Fig. 9, dexamethasone treatment did not significantly affect the levels of these two markers, suggesting that the observed positive effect of dexamethasone is independent of the autophagy process.

4. Discussion

We demonstrated that LD animals show reduced levels of HSF1 and their targets, and hence the compromised HSR could contribute to neuropathology in LD. We further demonstrated that pharmacological activation of HSF1, using dexamethasone, was able to partially restore levels of HSF1 and its targets. Indeed, high levels of HSPs are seen in long-lived animals (Morley and Morimoto, 2004; Singh et al., 2006; Salway et al., 2011), possibly as a response mechanism to help unfolded proteins regain their conformation. Since laforin and malin are essential for the induction of HSF1-mediated HSR (Sengupta et al., 2011), it could be suggested that the absence of laforin or malin leads to compromised unfolded protein response (UPR) (Vernia et al., 2009; Zeng et al., 2012) and eventual neurodegeneration in LD. Thus, the activation of HSR would have reduced abnormal protein load in laforin- or malin-deficient cells and helped their survival. Recent reports suggest crosstalk between the HSR pathway and the oxidative stress response pathway (Agarwal and Ganesh, 2020). Moreover, increased levels of HSPs confer protection against oxidative stress (Chionh et al., 2019). Consistent with this notion, we observed that the pharmacological activation of HSR reduces oxidative stress in LD models. Thus, compromised HSR might underlie oxidative stress in LD.

Neuroinflammation is well documented in LD models. Studies have shown the increased levels of inflammatory markers in both laforin- and malin-deficient animals (López-González et al., 2017; Rai et al., 2017). Intriguingly, dexamethasone treatment reduced levels of neuroinflammatory markers in LD animals. Dexamethasone, a corticosteroid, is known for its anti-inflammatory property and has been shown to

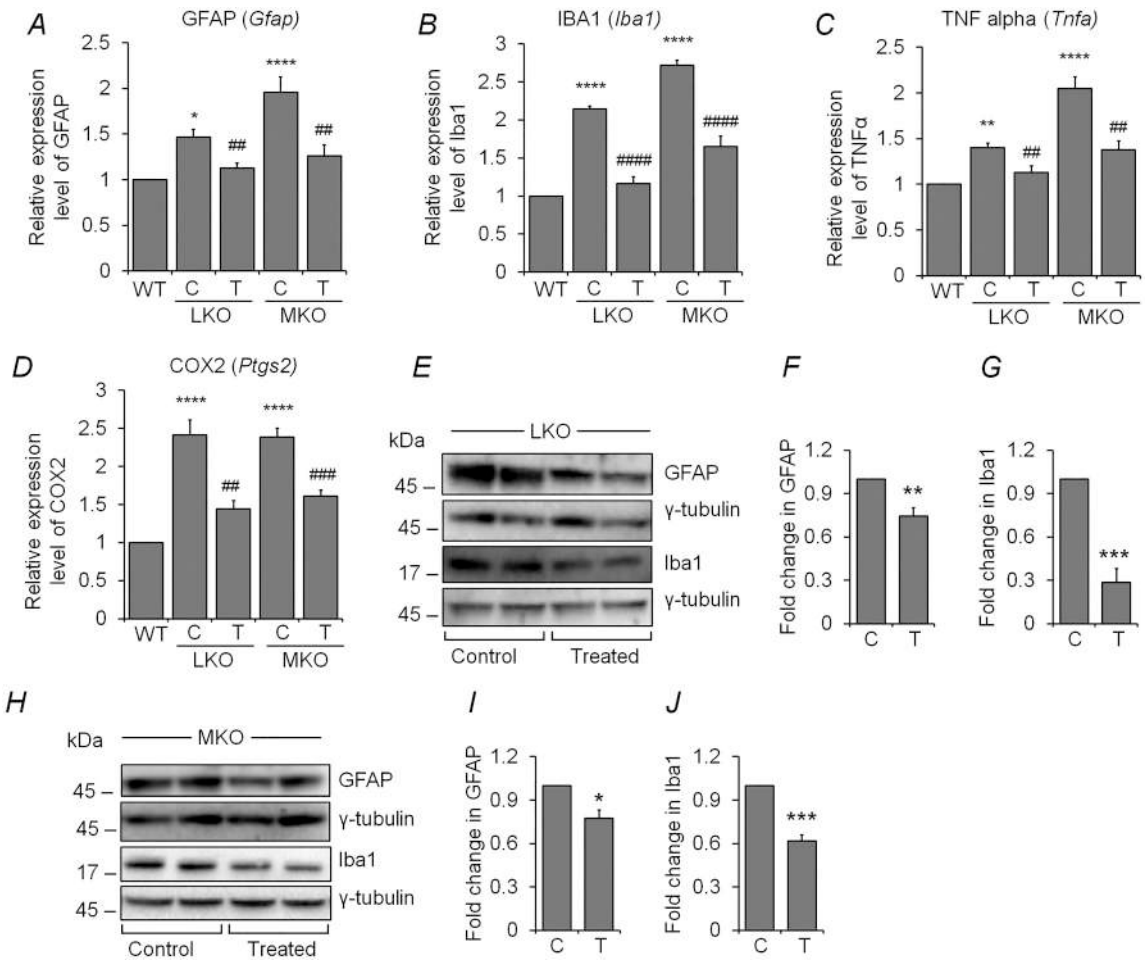

Fig. 5. Dexamethasone treatment reduces the level of neuroinflammatory markers in LD mice brains.
Bar diagrams showing the fold change in the expression levels of four neuroinflammatory markers *Gfap* (***A***), *Iba1* (***B***), *Tnfa* (***C***), and *Ptgs2* (***D***) in the brain tissues of the laforin-deficient (LKO) or malin-deficient mice (MKO), as compared to their wild-type littermates (WT). Similarly, the expression levels of these markers in the brain tissues of the control (identified as "[C]") and dexamethasone-treated (identified as "[T]") LD mouse models were also compared. Each bar represents the mean average (+ SEM); the statistical significance was calculated using an ordinary one-way ANOVA test (n = 6). Herein, asterisk refers to comparison with the wild-type untreated samples (* $p < 0.05$; ** $p < 0.01$; *** $p < 0.001$; **** $p < 0.0001$), and the hashtag refers to the comparison with the control sets (vehicle-treated; [C]) of the respective genotypes (## $p < 0.01$; ### $p < 0.001$; #### $p < 0.0001$). Representative images of the immunoblots showing the relative levels of GFAP, Iba1, and the loading control (γ -tubulin) in the whole brain lysates of the laforin- (LKO) (***E***) or malin-deficient mice (MKO) (***H***) as compared with the wild-type littermates. Bar diagrams showing the fold change in the signal intensities (measured by densitometric analysis) for GFAP in the dexamethasone-treated laforin-deficient mice (***F***) or malin-deficient mice (***I***) brain as compared with the control mice. Similarly, the fold change in the signal intensities for Iba1 in the dexamethasone-treated laforin-deficient mice (***G***) or malin-deficient mice (***J***) as compared with the control mice. The signals were normalized to the γ-tubulin level. Each bar (in ***F***, ***G***, ***I***, and ***J***) represent the mean average (+ SEM), and the statistical significance was calculated using Student's unpaired t-test (n = 3); asterisks denote statistically significant changes where * $p < 0.05$, ** $p < 0.01$, and *** $p < 0.001$.

control neuroinflammation in mice (Meneses et al., 2017). Dexamethasone, either alone or in combination, is also known to suppress epileptic seizures, possibly by suppressing the pro-inflammatory response (Pranzatelli and Tate, 2017; Guzzo et al., 2018; Vizuete et al., 2018; Garcia-Curran et al., 2019). Since neuroinflammation is linked to epileptic seizures (Vezzani et al., 2019), it is therefore possible that anti-inflammatory property of dexamethasone rescued the susceptibility to induced seizures in LD animals. It is equally likely that dexamethasone was able to suppress the inflammatory response by activating the HSR. HSR, being a pro-survival pathway, negatively regulates the neuroinflammatory response (Driedonks et al., 2015). For example, overexpression of HSP70 reduced the level of pro-inflammatory markers in a cellular model for Parkinson's disease (Yu et al., 2018). Therefore, it will be of interest to dissect the hierarchical regulation of inflammatory pathway *vis-a-vis* the HSR.

Lafora bodies are a hallmark of LD pathology. Studies, using mouse models, have shown that suppressing the formation of Lafora bodies reduces neuroinflammation and seizure susceptibility (Turnbull et al., 2011; Pederson et al., 2013; Rai et al., 2017). Therefore, it is intriguing to note that dexamethasone treatment rescued neuroinflammation and seizure susceptibility without significantly affecting the size or distribution of Lafora bodies in mouse models for LD. It is therefore plausible, that epileptic seizures are secondary to Lafora bodies and possibly due to neuroinflammation. Support for this notion comes from animal models of LD, wherein Lafora bodies are seen as early as one month after birth but spontaneous seizures are seen in 8-to-10-month-old animals (Ganesh et al., 2002; Criado et al., 2012; Duran et al., 2014). Thus, glycogen-rich aggregates in neurons can contribute to epileptic seizures. Indeed, a

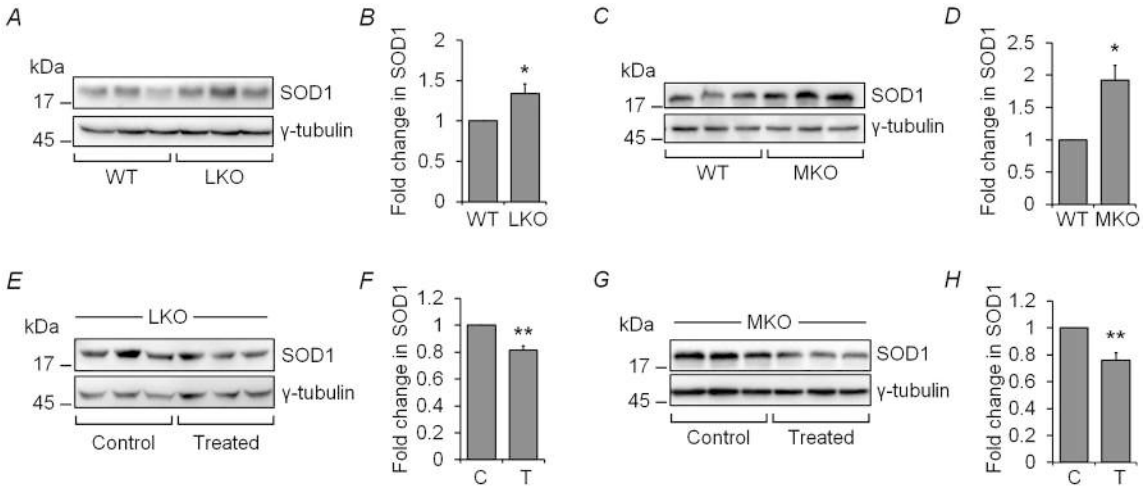

Fig. 6. Dexamethasone treatment reduces the SOD1 levels in LD mice brain Representative images of the immunoblots showing relative levels of SOD1 and the loading control (γ -tubulin) in the whole brain lysates of laforin- (LKO) (*A*) or malin-deficient mice (MKO) (*C*) as compared with the wild-type littermates and control and dexamethasone-treated animals that are deficient for laforin (LKO) (*E*) or malin (MKO) (*G*), as indicated. Bar diagram shows the fold change in the signal intensities (measured by densitometric analysis) for SOD1 in the laforin-deficient mice (*B*) or malin-deficient mice (*D*) brain as compared with the wild-type littermates and laforin-deficient mice (*F*) or malin-deficient mice (*H*) upon treatment with dexamethasone (identified as "T") as compared with the vehicle-treated controls (identified as "C)". The signals were normalized to the γ-tubulin level. Each bar (in *B*, *D*, *F*, and *H*) represent the mean average (+ SEM), and the statistical significance was calculated using Student's unpaired t-test (n = 3); asterisks denote statistically significant changes where * $p < 0.05$ and ** $p < 0.01$.

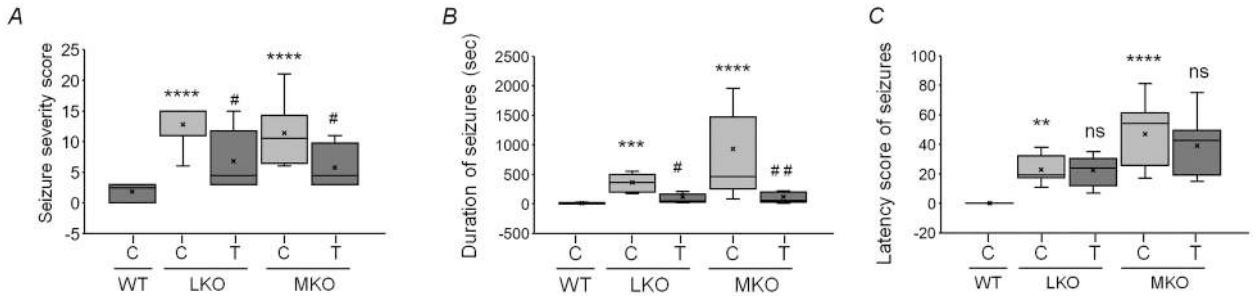

Fig. 7. Dexamethasone is protective against pentylenetetrazol-induced seizures.

higher incidence of epilepsy is noted in the elderly population (Olafsson et al., 2005; Leppik and Birnbaum, 2010) and aged brains are also known to harbor polyglucosan bodies - one form of glycogen aggregates very similar to Lafora bodies (Cavanagh, 1999; Rai and Ganesh, 2019). Therefore, it would be of interest to study the causal relation between Lafora bodies and epilepsy and to dissect molecular links between them. Nonetheless, the present study establishes a role for HSR in seizure susceptibility and neuroinflammation and dexamethasone as a potential antiepileptic agent, suitable for further studies in LD.

Author contributions

S.G and P·S conceived and designed the experiments; P.S. and B.V. performed the experiments; S.G., P.S., and B.V. analyzed the data; S.G. and P.S. wrote the paper; all authors reviewed the manuscript.

Funding

The study was supported by a sponsored research grant from the Department of Biotechnology, (Government of India), to SG (BT/HRD/35/01/01/2017). SG is PK Kelkar Endowed Chair at IIT Kanpur. PS and BV were supported by a research fellowship from the Ministry of Human Resource Development (Government of India), and the Council of Scientific & Industrial Research (Government of India), respectively.

Box plot showing the increased seizure severity, duration, and latency for the vehicle treated laforin- (LKO) or malin-deficient mice (MKO) as compared with the wild-type (WT) littermates and the protective effect of dexamethasone in reducing the seizure severity and duration in LD mouse models. "C" refers to vehicle treated control group, and "T" refers to the dexamethasone treatment group ($n = 12$ for all groups). The statistical significance was calculated using Kruskal-Wallis ANOVA on the RANKS test. Herein, asterisk refers to comparison with the wild-type untreated samples (** $p < 0.01$, *** $p < 0.001$, and **** $p < 0.0001$), and the hashtag refers to the comparison with the control sets (vehicle-treated; [C]) of the respective genotypes (# $p < 0.05$; ## $p < 0.01$; ns, not significant).

Declaration of Competing Interest

The sponsors had no involvement in study design, data collection, analysis and interpretation of data, writing of the manuscript or the decision to submit the article for publication. The authors declare that they have no conflict of interest.

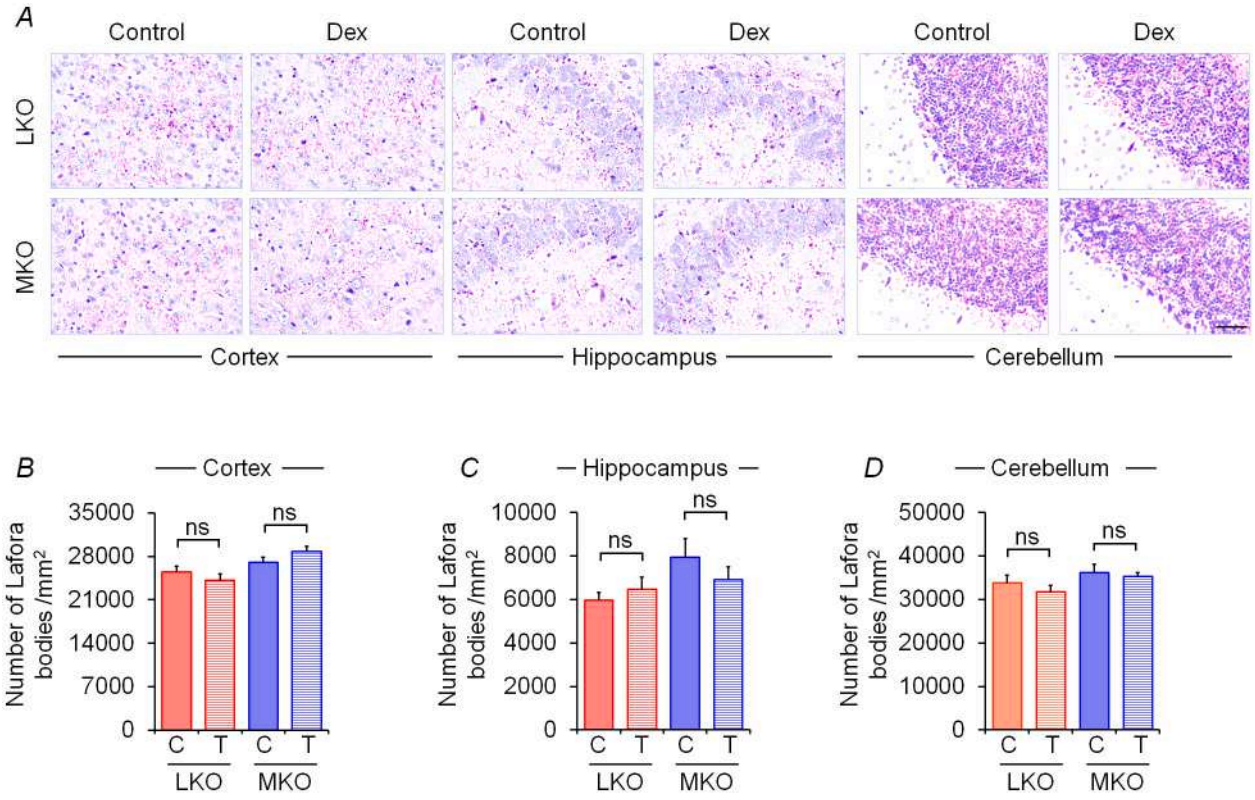

Fig. 8. Dexamethasone treatment does not affect Lafora body formation.
Representative images showing the distribution of PAS+ Lafora bodies in the cortex, hippocampus, and cerebellum (***A***) of the brain sections of the animals with the genotype as identified (LKO, laforin-deficient mice; MKO, malin-deficient mice) (scale bar = 50 μm). Bar diagrams (***B***, ***C***, and ***D***) showing the number of PAS+ Lafora bodies in the laforin-deficient mice and malin-deficient mice upon treatment with dexamethasone as compared with the untreated controls, as indicated. Each bar represents the mean average (+ SEM), and the statistical significance was determined using an ordinary one-way ANOVA test, but none were found to be statistically significant (n = 6).

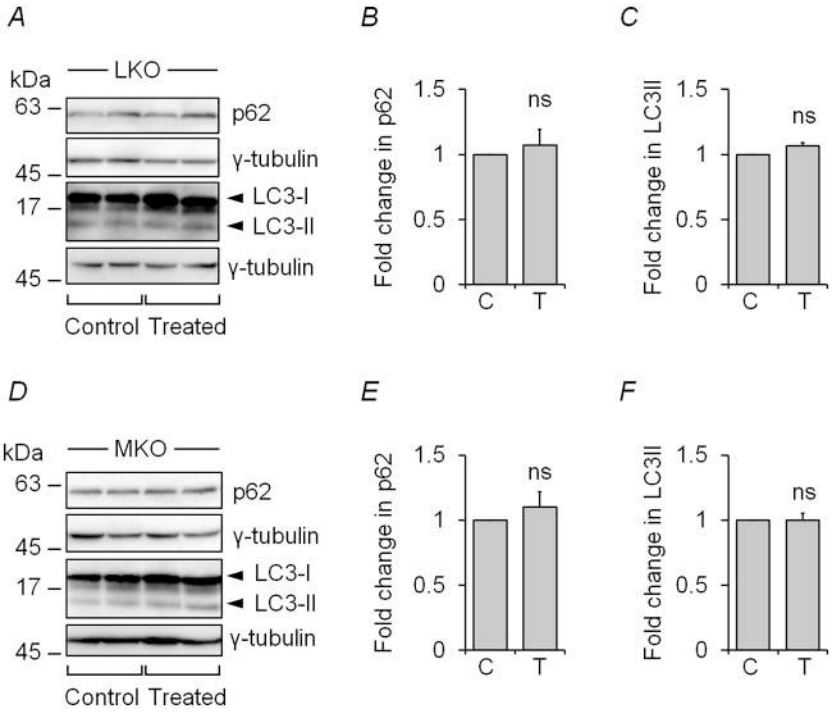

Fig. 9. Dexamethasone treatment has no effect on autophagy. Representative images of the immunoblots showing relative levels of autophagy markers p62 and LC3 and the loading control (γ -tubulin) in the brain lysate of control and dexamethasone-treated animals that are deficient for laforin (LKO) (***A***) or malin (MKO) (***D***), as indicated. Bar diagram showing the fold change in the signal intensities (measured by densitometric analysis) for p62 or LC3-II in the laforin-deficient mice (***B***, ***C***) or malin-deficient mice (***E***, ***F***) upon treatment with dexamethasone as compared with the untreated controls. The signals were normalized to the γ-tubulin level. Each bar (in ***B***, ***C***, ***E,*** and ***F***) represent the mean average (+ SEM), and the statistical significance was calculated using Student's unpaired t-test (n = 3) (* $p < 0.05$).

Acknowledgements

The authors thank Dr. Berge A. Minassian, currently at the UT Southwestern Medical Center, USA, for the gift of Lafora disease mouse models used in the study.

Appendix A. Supplementary data

Supplementary data to this article can be found online at https://doi.org/10.1016/j.expneurol.2021.113656.

References

Agarwal, S., Ganesh, S., 2020. Perinuclear mitochondrial clustering, increased ROS levels, and HIF1 are required for the activation of HSF1 by heat stress. J. Cell Sci. 133, jcs245589 https://doi.org/10.1242/jcs.245589.

Aguado, C., Sarkar, S., Korolchuk, V.I., Criado, O., Vernia, S., Boya, P., Sanz, P., Rodríguez de Córdoba, S., Knecht, E., Rubinsztein, D.C., 2010. Laforin, the most common protein mutated in Lafora disease, regulates autophagy. Hum. Mol. Genet. 19, 2867–2876. https://doi.org/10.1093/hmg/ddq190.

Barna, J., Csermely, P., Vellai, T., 2018. Roles of heat shock factor 1 beyond the heat shock response. Cell. Mol. Life Sci. 75, 2897–2916. https://doi.org/10.1007/s00018-018-2836-6.

Beere, H.M., 2004. "the stress of dying": the role of heat shock proteins in the regulation of apoptosis. J. Cell Sci. 117, 2641–2651. https://doi.org/10.1242/jcs.01284.

Calderwood, S.K., Murshid, A., Prince, T., 2009. The shock of aging: molecular chaperones and the heat shock response in longevity and aging–a mini-review. Gerontology. 55, 550–558. https://doi.org/10.1159/000225957.

Cavanagh, J.B., 1999. Corpora-amylacea and the family of polyglucosan diseases. Brain Res. Brain Res. Rev. 29, 265–295. https://doi.org/10.1016/s0165-0173(99)00003-x.

Chan, E.M., Young, E.J., Ianzano, L., Munteanu, I., Zhao, X., Christopoulos, C.C., Avanzini, G., Elia, M., Ackerley, C.A., Jovic, N.J., Bohlega, S., Andermann, E., Rouleau, G.A., Delgado-Escueta, A.V., Minassian, B.A., Scherer, S.W., 2003. Mutations in NHLRC1 cause progressive myoclonus epilepsy. Nat. Genet. 35, 125–127. https://doi.org/10.1038/ng1238.

Chionh, Y.T., Cui, J., Koh, J., Mendenhall, I.H., Ng, J.H.J., Low, D., Itahana, K., Irving, A. T., Wang, L.F., 2019. High basal heat-shock protein expression in bats confers resistance to cellular heat/oxidative stress. Cell Stress Chaperones 24, 835–849. https://doi.org/10.1007/s12192-019-01013-y.

Creagh, E.M., Sheehan, D., Cotter, T.G., 2000. Heat shock proteins–modulators of apoptosis in tumour cells. Leukemia. 14, 1161–1173. https://doi.org/10.1038/sj.leu.2401841.

Criado, O., Aguado, C., Gayarre, J., Duran-Trio, L., Garcia-Cabrero, A.M., Vernia, S., Millán, B.S., Heredia, M., Romá-Mateo, C., Mouron, S., Juana-López, L., Domínguez, M., Navarro, C., Serratosa, J.M., Sanchez, M., Sanz, P., Bovolenta, P., Knecht, E., Rodriguez de Cordoba, S., 2012. Lafora bodies and neurological defects in Malin-deficient mice correlate with impaired autophagy [published correction appears in Hum. Mol. Genet. 2012 Oct 1;21(19):4366]. Hum. Mol. Genet. 21, 1521–1533. https://doi.org/10.1093/hmg/ddr590.

Cummings, C.J., Mancini, M.A., Antalffy, B., DeFranco, D.B., Orr, H.T., Zoghbi, H.Y., 1998. Chaperone suppression of aggregation and altered subcellular proteasome localization imply protein misfolding in SCA1. Nat. Genet. 19, 148–154. https://doi.org/10.1038/502.

Dai, C., 2018. The heat-shock, or HSF1-mediated proteotoxic stress, response in cancer: from proteomic stability to oncogenesis. Philos. Trans. R. Soc. Lond. Ser. B Biol. Sci. 373 https://doi.org/10.1098/rstb.2016.0525.

Driedonks, N., Xu, J., Peters, J.L., Park, S., Rieu, I., 2015. Multi-level interactions between heat shock factors, heat shock proteins, and the redox system regulate acclimation to heat. Front. Plant Sci. 6, 999. https://doi.org/10.3389/fpls.2015.00999.

Dukay, B., Csoboz, B., Tóth, M.E., 2019. Heat-shock proteins in Neuroinflammation. Front. Pharmacol. 10 https://doi.org/10.3389/fphar.2019.00920.

Duran, J., Gruart, A., García-Rocha, M., Delgado-García, J.M., Guinovart, J.J., 2014. Glycogen accumulation underlies neurodegeneration and autophagy impairment in Lafora disease. Hum. Mol. Genet. 23, 3147–3156. https://doi.org/10.1093/hmg/ddu024.

Ganesh, S., Agarwala, K.L., Ueda, K., Akagi, T., Shoda, K., Usui, T., Hashikawa, T., Osada, H., Delgado-Escueta, A.V., Yamakawa, K., 2000. Laforin, defective in the progressive myoclonus epilepsy of Lafora type, is a dual-specificity phosphatase associated with polyribosomes. Hum. Mol. Genet. 9, 2251–2261. https://doi.org/10.1093/oxfordjournals.hmg.a018916.

Ganesh, S., Delgado-Escueta, A.V., Sakamoto, T., Avila, M.R., Machado-Salas, J., Hoshii, Y., Akagi, T., Gomi, H., Suzuki, T., Amano, K., Agarwala, K.L., Hasegawa, Y., Bai, D.S., Ishihara, T., Hashikawa, T., Itohara, S., Cornford, E.M., Niki, H., Yamakawa, K., 2002. Targeted disruption of the Epm2a gene causes formation of Lafora inclusion bodies, neurodegeneration, ataxia, myoclonus epilepsy and impaired behavioral response in mice. Hum. Mol. Genet. 11, 1251–1262. https://doi.org/10.1093/hmg/11.11.1251.

García-Cabrero, A.M., Marinas, A., Guerrero, R., de Córdoba, S.R., Serratosa, J.M., Sánchez, M.P., 2012. Laforin and Malin deletions in mice produce similar neurologic impairments. J. Neuropathol. Exp. Neurol. 71, 413–421. https://doi.org/10.1097/NEN.0b013e318253350f.

García-Cabrero, A.M., Sánchez-Elexpuru, G., Serratosa, J.M., Sánchez, M.P., 2014. Enhanced sensitivity of laforin- and Malin-deficient mice to the convulsant agent pentylenetetrazole. Front. Neurosci. 8 https://doi.org/10.3389/fnins.2014.00291.

Garcia-Curran, M.M., Hall, A.M., Patterson, K.P., Shao, M., Eltom, N., Chen, K., Dubé, C. M., Baram, T.Z., 2019. Dexamethasone attenuates hyperexcitability provoked by experimental febrile status epilepticus. eNeuro 6. https://doi.org/10.1523/ENEURO.0430-19.2019. ENEURO.0430-19.2019.

Garyali, P., Siwach, P., Singh, P.K., Puri, R., Mittal, S., Sengupta, S., Parihar, R., Ganesh, S., 2009. The Malin-laforin complex suppresses the cellular toxicity of misfolded proteins by promoting their degradation through the ubiquitin-proteasome system. Hum. Mol. Genet. 18, 688–700. https://doi.org/10.1093/hmg/ddn398.

Garyali, P., Segvich, D.M., DePaoli-Roach, A.A., Roach, P.J., 2014. Protein degradation and quality control in cells from laforin and Malin knockout mice. J. Biol. Chem. 289, 20606–20614. https://doi.org/10.1074/jbc.M114.580167.

Gentry, M.S., Worby, C.A., Dixon, J.E., 2005. Insights into Lafora disease: Malin is an E3 ubiquitin ligase that ubiquitinates and promotes the degradation of laforin. Proc. Natl. Acad. Sci. U. S. A. 102, 8501–8506. https://doi.org/10.1073/pnas.0503285102.

Goenka, A., Parihar, R., Ganesh, S., 2018. Heat shock-induced transcriptional and translational arrest in mammalian cells. In: AAA, Ed Asea, Kaur, P. (Eds.), Heat Shock Proteins and Stress. Springer International Publishing AG, Cham, pp. 267–280.

Guzzo, E.F.M., Lima, K.R., Vargas, C.R., Coitinho, A.S., 2018. Effect of dexamethasone on seizures and inflammatory profile induced by kindling seizure model. J. Neuroimmunol. 325, 92–98. https://doi.org/10.1016/j.jneuroim.2018.10.005.

Hansson, O., Nylandsted, J., Castilho, R.F., Leist, M., Jäättelä, M., Brundin, P., 2003. Overexpression of heat shock protein 70 in R6/2 Huntington's disease mice has only modest effects on disease progression. Brain Res. 970, 47–57. https://doi.org/10.1016/s0006-8993(02)04275-0.

Hay, D.G., Sathasivam, K., Tobaben, S., Stahl, B., Marber, M., Mestril, R., Mahal, A., Smith, D.L., Woodman, B., Bates, G.P., 2004. Progressive decrease in chaperone protein levels in a mouse model of Huntington's disease and induction of stress proteins as a therapeutic approach. Hum. Mol. Genet. 13, 1389–1405. https://doi.org/10.1093/hmg/ddh144.

Howarth, J.L., Kelly, S., Keasey, M.P., Glover, C.P.J., Lee, Y.-B., Mitrophanous, K., Chapple, J.P., Gallo, J.M., Cheetham, M.E., Uney, J.B., 2007. Hsp40 molecules that target to the ubiquitin-proteasome system decrease inclusion formation in models of polyglutamine disease. Mol. Ther. 15, 1100–1105. https://doi.org/10.1038/sj.mt.6300163.

Jain, N., Rai, A., Mishra, R., Ganesh, S., 2017. Loss of Malin, but not laforin, results in compromised autophagic flux and proteasomal dysfunction in cells exposed to heat shock. Cell Stress Chaperones 22, 307–315. https://doi.org/10.1007/s12192-016-0754-9.

Jana, N.R., Tanaka, M., Wang, Gh., Nukina, N., 2000. Polyglutamine length-dependent interaction of Hsp40 and Hsp70 family chaperones with truncated N-terminal huntingtin: their role in suppression of aggregation and cellular toxicity. Hum. Mol. Genet. 9, 2009–2018. https://doi.org/10.1093/hmg/9.13.2009.

Kakkar, V., Meister-Broekema, M., Minoia, M., Carra, S., Kampinga, H.H., 2014. Barcoding heat shock proteins to human diseases: looking beyond the heat shock response. Dis. Model. Mech. 7, 421–434. https://doi.org/10.1242/dmm.014563.

Kato, K., Katoh-Semba, R., Takeuchi, I.K., Ito, H., Kamei, K., 1999. Responses of heat shock proteins hsp27, alphaB-crystallin, and hsp70 in rat brain after kainic acid-induced seizure activity. J. Neurochem. 73, 229–236. https://doi.org/10.1046/j.1471-4159.1999.0730229.x.

Kennedy, D., Jäger, R., Mosser, D.D., Samali, A., 2014. Regulation of apoptosis by heat shock proteins. IUBMB Life 66, 327–338. https://doi.org/10.1002/iub.1274.

Knop, L.A., Shintcovsk, R.L., Retamoso, L.B., Ribeiro, J.S., Tanaka, O.M., 2012. Non-steroidal and steroidal anti-inflammatory use in the context of orthodontic movement. Eur. J. Orthod. 34, 531–535. https://doi.org/10.1093/ejo/cjq173.

Knowlton, A.A., Sun, L., 2001. Heat-shock factor-1, steroid hormones, and regulation of heat-shock protein expression in the heart. Am. J. Physiol. Heart Circ. Physiol. 280, H455–H464. https://doi.org/10.1152/ajpheart.2001.280.1.H455.

Laane, E., Tamm, K.P., Buentke, E., Ito, K., Kharaziha, P., Oscarsson, J., Corcoran, M., Björklund, A.-C., Hultenby, K., Lundin, J., Heyman, M., Söderhäll, S., Mazur, J., Porwit, A., Pandolfi, P.P., Zhivotovsky, B., Panaretakis, T., Grandér, D., 2009. Cell death induced by dexamethasone in lymphoid leukemia is mediated through initiation of autophagy [published correction appears in cell death differ. 2009 Jul; 16(7):1071. Khahariza, P [corrected to Kharaziha, P]]. Cell Death Differ. 16, 1018–1029. https://doi.org/10.1038/cdd.2009.46.

Le Breton, L., Mayer, M.P., 2016. A model for handling cell stress. Elife. 5, e22850 https://doi.org/10.7554/eLife.22850.

Leak, R.K., 2014. Heat shock proteins in neurodegenerative disorders and aging. J. Cell Commun. Signal. 8, 293–310. https://doi.org/10.1007/s12079-014-0243-9.

Leppik, I.E., Birnbaum, A.K., 2010. Epilepsy in the elderly. Ann. N. Y. Acad. Sci. 1184, 208–224. https://doi.org/10.1111/j.1749-6632.2009.05113.x.

López-González, I., Viana, R., Sanz, P., Ferrer, I., 2017. Inflammation in Lafora disease: evolution with disease progression in Laforin and Malin Knock-out mouse Models. Mol. Neurobiol. 54, 3119–3130. https://doi.org/10.1007/s12035-016-9884-4.

Maheshwari, M., Bhutani, S., Das, A., Mukherjee, R., Sharma, A., Kino, Y., Nukina, N., Jana, N.R., 2014. Dexamethasone induces heat shock response and slows down disease progression in mouse and fly models of Huntington's disease. Hum. Mol. Genet. 23, 2737–2751. https://doi.org/10.1093/hmg/ddt667.

Meneses, G., Gevorkian, G., Florentino, A., Bautista, M.A., Espinosa, A., Acero, G., Díaz, G., Fleury, A., Osorio, I.N.P., Rey, A.D., Fragoso, G., Sciutto, E., Besedovsky, H., 2017. Intranasal delivery of dexamethasone efficiently controls LPS-induced murine neuroinflammation. Clin. Exp. Immunol. 190, 304–314. https://doi.org/10.1111/cei.13018.

Minassian, B.A., Lee, J.R., Herbrick, J.A., Huizenga, J., Soder, S., Mungall, A.J., Dunham, I., Gardner, R., Fong, C.Y., Carpenter, S., Jardim, L., Satishchandra, P., Andermann, E., Snead 3rd, O.C., Lopes-Cendes, I., Tsui, L.C., Delgado-Escueta, A.V., Rouleau, G.A., Scherer, S.W., 1998. Mutations in a gene encoding a novel protein tyrosine phosphatase cause progressive myoclonus epilepsy. Nat. Genet. 20, 171–174. https://doi.org/10.1038/2470.

Mitsuno, S., Takahashi, M., Gondo, T., Hoshii, Y., Hanai, N., Ishihara, T., Yamada, M., 1999. Immunohistochemical, conventional and immunoelectron microscopical characteristics of periodic acid-Schiff-positive granules in the mouse brain. Acta Neuropathol. 98, 31–38. https://doi.org/10.1007/s004010051048.

Mittal, S., Ganesh, S., 2010. Protein quality control mechanisms and neurodegenerative disorders: checks, balances and deadlocks. Neurosci. Res. 68, 159–166. https://doi.org/10.1016/j.neures.2010.08.002.

Mittal, S., Dubey, D., Yamakawa, K., Ganesh, S., 2007. Lafora disease proteins Malin and laforin are recruited to aggresomes in response to proteasomal impairment. Hum. Mol. Genet. 16, 753–762. https://doi.org/10.1093/hmg/ddm006.

Molitoris, J.K., McColl, K.S., Swerdlow, S., Matsuyama, M., Lam, M., Finkel, T.H., Matsuyama, S., Distelhorst, C.W., 2011. Glucocorticoid elevation of dexamethasone-induced gene 2 (Dig2/RTP801/REDD1) protein mediates autophagy in lymphocytes [published correction appears in J. Biol. Chem. 2011 Nov 11;286(45):39673]. J. Biol. Chem. 286, 30181–30189. https://doi.org/10.1074/jbc.M111.245423.

Morley, J.F., Morimoto, R.I., 2004. Regulation of longevity in *Caenorhabditis elegans* by heat shock factor and molecular chaperones. Mol. Biol. Cell 15, 657–664. https://doi.org/10.1091/mbc.e03-07-0532.

Olafsson, E., Ludvigsson, P., Gudmundsson, G., Hesdorffer, D., Kjartansson, O., Hauser, W.A., 2005. Incidence of unprovoked seizures and epilepsy in Iceland and assessment of the epilepsy syndrome classification: a prospective study. Lancet Neurol. 4, 627–634. https://doi.org/10.1016/S1474-4422(05)70172-1.

Parihar, R., Rai, A., Ganesh, S., 2018. Lafora disease: from genotype to phenotype. J. Genet. 97, 611–624. https://doi.org/10.1007/s12041-018-0949-1.

Pederson, B.A., Turnbull, J., Epp, J.R., Weaver, S.A., Zhao, X., Pencea, N., Roach, P.J., Frankland, P.W., Ackerley, C.A., Minassian, B.A., 2013. Inhibiting glycogen synthesis prevents Lafora disease in a mouse model. Ann. Neurol. 74, 297–300. https://doi.org/10.1002/ana.23899.

Pockley, A.G., 2002. Heat shock proteins, inflammation, and cardiovascular disease. Circulation. 105, 1012–1017. https://doi.org/10.1161/hc0802.103729.

Pranzatelli, MR., Tate, ED., 2017. Dexamethasone, intravenous immunoglobulin, and rituximab combination immunotherapy for pediatric Opsoclonus-myoclonus syndrome [published correction appears in Pediatr Neurol. 2017 Nov 20:]. Pediatr. Neurol. 73, 48–56. doi:https://doi.org/10.1016/j.pediatrneurol.2017.04.027.

Puri, R., Suzuki, T., Yamakawa, K., Ganesh, S., 2012. Dysfunctions in endosomal-lysosomal and autophagy pathways underlie neuropathology in a mouse model for Lafora disease. Hum. Mol. Genet. 21, 175–184. https://doi.org/10.1093/hmg/ddr452.

Rai, A., Ganesh, S., 2019. Polyglucosan bodies in aged brain and neurodegeneration: Cause or consequence? In: Rath, P.C. (Ed.), Models, Molecules and Mechanisms in Biogerontology. Springer Nature Singapore Pte Ltd, Singapore, pp. 57–89.

Rai, A., Mishra, R., Ganesh, S., 2017. Suppression of leptin signaling reduces polyglucosan inclusions and seizure susceptibility in a mouse model for Lafora disease. Hum. Mol. Genet. 26, 4778–4785. https://doi.org/10.1093/hmg/ddx357.

Romá-Mateo, C., Aguado, C., García-Giménez, J.L., Ibáñez-Cabellos, J.S., Seco-Cervera, M., Pallardó, F.V., Knecht, E., Sanz, P., 2015a. Increased oxidative stress and impaired antioxidant response in Lafora disease. Mol. Neurobiol. 51, 932–946. https://doi.org/10.1007/s12035-014-8747-0.

Romá-Mateo, C., Aguado, C., García-Giménez, J.L., Knecht, E., Sanz, P., Pallardó, F.V., 2015b. Oxidative stress, a new hallmark in the pathophysiology of Lafora progressive myoclonus epilepsy. Free Radic. Biol. Med. 88, 30–41. https://doi.org/10.1016/j.freeradbiomed.2015.01.034.

Saibil, H., 2013. Chaperone machines for protein folding, unfolding and disaggregation. Nat. Rev. Mol. Cell Biol. 14, 630–642. https://doi.org/10.1038/nrm3658.

Salway, K.D., Gallagher, E.J., Page, M.M., Stuart, J.A., 2011. Higher levels of heat shock proteins in longer-lived mammals and birds. Mech. Ageing Dev. 132, 287–297. https://doi.org/10.1016/j.mad.2011.06.002.

Sengupta, S., Badhwar, I., Upadhyay, M., Singh, S., Ganesh, S., 2011. Malin and laforin are essential components of a protein complex that protects cells from thermal stress. J. Cell Sci. 124, 2277–2286. https://doi.org/10.1242/jcs.082800.

Singh, P.K., Singh, S., Ganesh, S., 2013. Activation of serum/glucocorticoid-induced kinase 1 (SGK1) underlies increased glycogen levels, mTOR activation, and autophagy defects in Lafora disease [published correction appears in Mol. Biol. Cell. 2014 May;25(9):1543]. Mol. Biol. Cell 24, 3776–3786. https://doi.org/10.1091/mbc.E13-05-0261.

Singh, R., Kølvraa, S., Bross, P., Christensen, K., Gregersen, N., Tan, Q., Jensen, U.B., Eiberg, H., Rattan, S.I.R., 2006. Heat-shock protein 70 genes and human longevity: a view from Denmark. Ann. N. Y. Acad. Sci. 1067, 301–308. https://doi.org/10.1196/annals.1354.040.

Singh, S., Ganesh, S., 2009. Lafora progressive myoclonus epilepsy: a meta-analysis of reported mutations in the first decade following the discovery of the EPM2A and NHLRC1 genes. Hum. Mutat. 30, 715–723. https://doi.org/10.1002/humu.20954.

Sinha, P., Verma, B., Ganesh, S., 2020. Trehalose ameliorates seizure susceptibility in Lafora disease mouse models by suppressing neuroinflammation and endoplasmic reticulum stress. Mol. Neurobiol. https://doi.org/10.1007/s12035-020-02170-3.

Striano, P., Zara, F., Turnbull, J., Girard, J.M., Ackerley, C.A., Cervasio, M., Rosa, G.D., Basso-De Caro, M.L., Striano, S., Minassian, B.A., 2008. Typical progression of myoclonic epilepsy of the Lafora type: a case report. Nat. Clin. Pract. Neurol. 4, 106–111. https://doi.org/10.1038/ncpneuro0706.

Sun, L., Chang, J., Kirchhoff, S.R., Knowlton, A.A., 2000. Activation of HSF and selective increase in heat-shock proteins by acute dexamethasone treatment. Am. J. Physiol. Heart Circ. Physiol. 278, H1091–H1097. https://doi.org/10.1152/ajpheart.2000.278.4.H1091.

Sweeney, P., Park, H., Baumann, M., Dunlop, J., Frydman, J., Kopito, R., McCampbell, A., Leblanc, G., Venkateswaran, Nurmi A., Hodgson, R., 2017. Protein misfolding in neurodegenerative diseases: implications and strategies. Transl. Neurodegener. 6, 6. https://doi.org/10.1186/s40035-017-0077-5.

Tagliabracci, V.S., Turnbull, J., Wang, W., Girard, J.M., Zhao, X., Skurat, A.V., Delgado-Escueta, A.V., Minassian, B.A., Depaoli-Roach, A.A., Roach, P.J., 2007. Laforin is a glycogen phosphatase, deficiency of which leads to elevated phosphorylation of glycogen in vivo. Proc. Natl. Acad. Sci. U. S. A. 104, 19262–19266. https://doi.org/10.1073/pnas.0707952104.

Tonkiss, J., Calderwood, S.K., 2005. Regulation of heat shock gene transcription in neuronal cells. Int. J. Hyperth. 21, 433–444. https://doi.org/10.1080/02656730500165514.

Tukaj, S., Kaminski, M., 2019. Heat shock proteins in the therapy of autoimmune diseases: too simple to be true? Cell Stress Chaperones 24, 475–479. https://doi.org/10.1007/s12192-019-01000-3.

Turnbull, J., Wang, P., Girard, J.M., Ruggieri, A., Wang, T.J., Draginov, A.G., Kameka, A. P., Pencea, N., Zhao, X., Ackerley, C.A., Minassian, B.A., 2010. Glycogen hyperphosphorylation underlies lafora body formation. Ann. Neurol. 68, 925–933. https://doi.org/10.1002/ana.22156.

Turnbull, J., DePaoli-Roach, A.A., Zhao, X., Cortez, M.A., Pencea, N., Tiberia, E., Piliguian, M., Roach, P.J., Wang, P., Ackerley, C.A., Minassian, B.A., 2011. PTG depletion removes Lafora bodies and rescues the fatal epilepsy of Lafora disease. PLoS Genet. 7, e1002037 https://doi.org/10.1371/journal.pgen.1002037.

Turnbull, J., Girard, J.M., Lohi, H., Chan, E.M., Wang, P., Tiberia, E., Omer, S., Ahmed, M., Bennett, C., Chakrabarty, A., Tyagi, A., Liu, Y., Pencea, N., Zhao, X., Scherer, S.W., Ackerley, C.A., Minassian, B.A., 2012. Early-onset Lafora body disease. Brain. 135, 2684–2698. https://doi.org/10.1093/brain/aws205.

Turnbull, J., Epp, J.R., Goldsmith, D., Zhao, X., Pencea, N., Wang, P., Frankland, P.W., Ackerley, C.A., Minassian, B.A., 2014. PTG protein depletion rescues malin-deficient Lafora disease in mouse. Ann. Neurol. 75, 442–446. https://doi.org/10.1002/ana.24104.

Turnbull, J., Tiberia, E., Striano, P., Genton, P., Carpenter, S., Ackerley, C.A., Minassian, B.A., 2016. Lafora disease. Epileptic Disord. 18, 38–62. https://doi.org/10.1684/epd.2016.0842.

Vabulas, R.M., Raychaudhuri, S., Hayer-Hartl, M., Hartl, F.U., 2010. Protein folding in the cytoplasm and the heat shock response. Cold Spring Harb. Perspect. Biol. 2, a004390. https://doi.org/10.1101/cshperspect.a004390.

Verghese, J., Abrams, J., Wang, Y., Morano, K.A., 2012. Biology of the heat shock response and protein chaperones: budding yeast (*Saccharomyces cerevisiae*) as a model system. Microbiol. Mol. Biol. Rev. 76, 115–158. https://doi.org/10.1128/MMBR.05018-11.

Vernia, S., Rubio, T., Heredia, M., Rodríguez de Córdoba, S., Sanz, P., 2009. Increased endoplasmic reticulum stress and decreased proteasomal function in lafora disease models lacking the phosphatase laforin. PLoS One 4, e5907. https://doi.org/10.1371/journal.pone.0005907.

Vezzani, A., Balosso, S., Ravizza, T., 2019. Neuroinflammatory pathways as treatment targets and biomarkers in epilepsy. Nat. Rev. Neurol. 15, 459–472. https://doi.org/10.1038/s41582-019-0217-x.

Vizuete, A.F.K., Hansen, F., Negri, E., Leite, M.C., de Oliveira, D.L., Gonçalves, C.A., 2018. Effects of dexamethasone on the Li-pilocarpine model of epilepsy: protection against hippocampal inflammation and astrogliosis. J. Neuroinflammation 15, 68. https://doi.org/10.1186/s12974-018-1109-5.

Warrick, J.M., Chan, H.Y., Gray-Board, G.L., Chai, Y., Paulson, H.L., Bonini, N.M., 1999. Suppression of polyglutamine-mediated neurodegeneration in Drosophila by the molecular chaperone HSP70. Nat. Genet. 23, 425–428. https://doi.org/10.1038/70532.

Wyttenbach, A., Sauvageot, O., Carmichael, J., Diaz-Latoud, C., Arrigo, A.P., Rubinsztein, D.C., 2002. Heat shock protein 27 prevents cellular polyglutamine toxicity and suppresses the increase of reactive oxygen species caused by huntingtin. Hum. Mol. Genet. 11, 1137–1151. https://doi.org/10.1093/hmg/11.9.1137.

Yamanaka, T., Miyazaki, H., Oyama, F., Kurosawa, M., Washizu, C., Doi, H., Nukina, N., 2008. Mutant Huntingtin reduces HSP70 expression through the sequestration of NF-Y transcription factor. EMBO J. 27, 827–839. https://doi.org/10.1038/emboj.2008.23.

Yu, W.W., Cao, S.N., Zang, C.X., Wang, L., Yang, H.Y., Bao, X.Q., Zhang, D., 2018. Heat shock protein 70 suppresses neuroinflammation induced by α-synuclein in astrocytes. Mol. Cell. Neurosci. 86, 58–64. https://doi.org/10.1016/j.mcn.2017.11.013.

Zeng, L., Wang, Y., Baba, O., Zheng, P., Liu, Y., Liu, Y., 2012. Laforin is required for the functional activation of Malin in endoplasmic reticulum stress resistance in neuronal cells. FEBS J. 279, 2467–2478. https://doi.org/10.1111/j.17424658.2012.08627.x.

Zhou, R., Sun, X., Li, Y., Huang, Q., Qu, Y., Mu, D., Li, X., 2019. Low-dose dexamethasone increases autophagy in cerebral cortical neurons of juvenile rats with Sepsis associated encephalopathy. Neuroscience. 419, 83–99. https://doi.org/10.1016/j.neuroscience.2019.09.020.